

Heat Transfer from an Immersed Heater in Liquid – Liquid – Solid Fluidized Beds

Dr. Balasim A. Abid *, Majid I. Abdul-Wahab ** & Asrar A. Al-Obaidy**

Received on:30/6/2008

Accepted on:2/4/2009

Abstract

Heat transfer from an immersed heating surface to a liquid-solid and liquid-liquid-solid fluidized beds have been studied. The experiments were carried out in a (0.22) m column diameter fitted with an axially mounted cylindrical heater heated electrically. The fluidizing medium was water as the continuous phase and kerosene as the dispersed phase. Low density (Polymethyl-methacrylate) particles were used. Previous published heat transfer correlations, obtained for fluidized beds containing high-density particles, gave significant deviations compared with the present data. New correlations were developed to predict the heat transfer coefficients in liquid-solid and liquid-liquid-solid fluidized beds. The new correlation is,

$$Nu = 0.164(Re_l Pr)^{1.56} (Re_d)^{4.05} (1 - e)^{6.96}$$

The heat transfer coefficients obtained from the present work were compared with those estimated from other correlations reported in the literature. The comparison shows a good agreement with the data obtained for the gas-liquid-solid fluidized beds using low-density particles.

انتقال الحرارة في أبراج التميع (سائل - سائل - صلب) لسطح تسخين مغمور

الخلاصة

يتضمن البحث دراسة عملية انتقال الحرارة في أبراج التميع ثلاثية الطور (سائل - سائل - صلب) باستخدام جسيمات صلبة واطئة الكثافة وسطح تسخين مغمور في داخل الطبقة المحيطة، وقد أجريت التجارب في عمود زجاجي ذو قطر داخلي مقداره (0.22) متر وباستخدام مسخن اسطواني مسخن كهربائياً ومثبت في وسط البرج. تمت دراسة تأثير معدل جريان كل من السائل الأول (الطور المستمر) والسائل الثاني (الطور المنتشر) على معاملات انتقال الحرارة في الأبراج المميعة. كذلك تم حل المعادلات التفاضلية التي تحكم عملية انتقال الحرارة في الطبقة المميعة باستخدام طريقة الفروق المحددة (Finite Difference) حيث تم إيجاد التوزيع القطري و المحوري لدرجات الحرارة داخل الطبقة المميعة وكذلك إيجاد قيم معامل التوصيل الحراري القطري المؤثر.

تم تحليل النتائج المستخلصة وفق نموذج المقاومات الحرارية (Thermal Resistances Model) وقد وجد إن المقاومة الداخلية للطبقة المميعة ذات قيمة كبيرة نسبياً في الطبقة الثنائية الطور (سائل - صلب) لكنها تقل عند إدخال الطور الثالث. تم تحليل النتائج إحصائياً لإيجاد معاملات انتقال الحرارة

* Chemical Engineering Department, University of Technology/Baghdad

** Chemical Engineering Department, Collage of Baghdad, University of Baghdad/Baghdad

بدلالة رقم نسلت (Nu Number) ورقم رينولدز (Re Number) ورقم براندتل (Pr Number) والمحتوى الحجمي للجسيمات الصلبة (Solid Holdup) للطبقة ثلاثية الطور سائل – سائل – صلب و كما يلي:

$$Nu = 0.164(Re_l Pr)^{1.56}(Re_d)^{4.05}(1 - e)^{6.96}$$

Keywords: Liquid-Liquid-Solid, Fluidized bed, Heat Transfer, Bed Porosity.

Nomenclature:

A , Cross sectional area of the bed, m^2 .
 C_p , Specific heat, J/kg. K.
 D_c , Column diameter, m.
 d_e , Equivalent hydraulic diameter of particle, m.
 d_p , Particle size (diameter), m.
 g , Acceleration due to gravity, m/s^2 .
 h , Overall heat transfer coefficient, W/m^2K .
 h_s , Heat transfer coefficient at the heater surface, W/m^2K .
 k_{er} , Effective radial thermal conductivity, W/m K.
 u_l , Superficial liquid velocity m/s.
 z , Axial distance, m.

Dimensionless Groups

Fr , Froud number (u^2 / gd_p).
 Nu , Particle Nusselt number (hd_p / K_l).
 Re , Reynolds number based on column diameter, ($r_l u D_c / m_l$).

Pr , Prandtl number in the radial direction, ($Cp_l m_l / k_l$).

Re'_l , Modified Reynolds numbers,

$$\left(\frac{u_l r d_p}{m_l (1 - e_l)} \right).$$

St Modified Stanton number in liquid-solid system $\left(\frac{h e_l}{Cp_l r_l u_l} \right)$.

St_m , Modified Stanton number in liquid-solid system, $\left(\frac{h e_l}{Cp_l r_l u_l} \right)$.

Pe , Modified Peclet number

$$\left[\frac{d_p u_l r_l Cp_l}{k_l (1 - e_l)} \right].$$

$$Pe_z, \left[\frac{GCpL}{k_{ez}} \right].$$

Greek Letters

e , Bed voidage.
 e_d , Dispersed phase holdup.
 e_c , Continuous phase holdup.
 e_s , Solid phase holdup.
 m , Viscosity of liquid, Pa.s
 r_l , Density of liquid, kg/m^3 .
 S_l , Surface tension of the liquid, N/m.
 n , Kinematic viscosity of liquid, m^2/s .

Subscripts

- c, Continuous phase.
- d, Dispersed phase.
- e, Effective.
- l, Liquid.
- r, Radial.

Introduction

Liquid-liquid-solid fluidized bed can be defined as a bed of particles fluidized by the co-current flow of two immiscible liquids in the bed. These types of fluidized beds are utilized recently as a solution to major problems taking place in bioreactors and in the development of an extractive fermentation process.

The studies on liquid-liquid-solid fluidized beds are generally limited in the literature. However, the hydrodynamic studies of liquid-liquid-solid fluidized beds tend to stimulate the operation with that of gas-liquid-solid fluidized beds because the mechanisms are expected to be the same. Several workers (Dakshinamurthy, et al. (1979), Dakshinamurthy, et al. (1984), Kim, et al. (1988), Kim, et al. (1989), Kim, et al. (1993) and Kim, et al. (1994)) studied the hydrodynamics of these beds and correlated the holdups, porosity as functions of the light and heavy liquids flow rates and to the particles diameters.

The traditional biotransformation processes are mostly performed in stirred tank reactors, in which the microorganisms and the desired product are suspended in an aqueous phase. After the biotransformation, the

product is recovered from the mixture by subsequent downstream processing.

This overall production manner, viz., batch biotransformation and subsequent downstream processing of the desired product, may result in a low overall productivity. Three problems may take place in this process; the first is when the substrate strongly decreases the production rate and a small amount of product is formed, the second problem is when the product inhibits biotransformation so that the amount of product is limited. The third problem facing some of these processes is in the biotransformations that suffer from unfavorable thermodynamic equilibrium, the case in which substrate is partially converted, and production halts due to the approach of thermodynamic equilibrium.

A possible solution to the problems mentioned above is direct removal of the product from the reaction environment (in case of product-inhibited or thermodynamically controlled biotransformation). In case of substrate-inhibited transformations, a controlled supply of substrate to the reaction phase can overcome the limited productivity. Supply can be arranged by using an organic solvent (liquid 1) with controlled supply of substrate (liquid 2) from a solid carrier (solid). Kinetic or thermodynamic product inhibition in bioconversion processes can be reduced by integrating the conversion with an extraction process in the liquid-liquid-solid fluidized bed. The catalyst can be freely suspended in a solid support.

The development of the advanced biological fluidized reactors which use light catalyst particles of densities range from 1050 to 1300 kg/m³ directed some of these studies towards the low-density particles fluidized beds. The studies began to project highlight upon the fundamental characteristics (hydrodynamics, heat and mass transfer) in three-phase fluidized beds containing low – density particles (Tang and Fan, 1990, Nore et al., 1992, Nore et al., 1994, Abdul Wahab, 1997 and Van Zeen, 2003).

The present study focused on the heat transfer characteristics of the low-density liquid- liquid- solid fluidized beds heated by immersed heater. A cylindrical shaped heater was used to study the heat transfer characteristics of these beds. The effects of continuous and dispersed liquid flow rates on the heat transfer resistance in the region adjacent to the heater surface and that in the bulk of the bed were examined experimentally. The equations describing the process were obtained and solved numerically by a finite difference technique. The solution of the energy equation gave the radial and axial temperature distributions for the whole fluidized bed over a wide range of operating conditions.

Experimental Work

The experimental work was performed using Q.V.F. glass test column of 0.22 m inside diameter and 2.25 m height. The column has a hemispherical bottom and consists of three sections, namely the working section,

accumulation section and the liquid outlet header. The overall combined height of these sections was 2.25 m.

The general arrangement of the equipment is shown in Fig.1 and the schematic diagram of the equipment is shown in Fig. 2. Working section of the column (1.0 m height) was located between the distributor and the accumulation section. Eight taps were used for mounting thermocouples axially. The taps were cemented to the column body using an adhesive (which has high thermal resistance) to prevent leakage. The accumulation section (0.7 m height) acted as a reservoir to accumulate large quantity of fluid.

The top of the accumulation section protruded into a concentrically mounted outlet header (which was a Perspex box of 0.25 m × 0.25 m × 0.75 m). The header thus acted as a weir over which the liquid flowed, thereby maintaining an approximately constant head in the column. The liquid exited from the outlet header through three hoses, which were valve to enable varying proportions of the flow to be either returned to the feed reservoir or sent to the drain.

Solid particles were supported on a perforated plate (like mesh) of spaced holes of 1 mm diameter, which served as a continuous phase distributor. The distributor was situated between the main column section and the entrance of the continuous phase which was introduced through a (2.54) cm pipe from liquid reservoir. Polymer (polymethyl-mthacrylate) particles (0.00317 m average diameter) were selected as packing.

The dispersed phase (kerosene) was fed to the column through a ring type distributor formed by a copper pipe of (0.01) m i.d. and (0.001) m thickness. Kerosene flows from the distributor through fifty- three holes of (0.002) m diameter each. The physical properties of the dispersed and continuous liquid phases are given in Table 1. The flow rates of the continuous and dispersed phase were measured by calibrated flow meters and regulated by means of globe valves on the feed and bypass lines.

The heater assembly (shown schematically in Fig. 3), was installed vertically at (30) cm above the distributor as a heat source in the immersed heater-to-bed system consisted of a copper cylinder of (0.065) m outside diameter and (0.4) m height. Two U-Shaped heating elements of (0.013) m diameter, (0.3) m length and (3000) W power (U shaped) were located in wells drilled inside the cylinder. The space between the heating elements and the cylinder was filled with lubricating oil to give a good heat distribution and to prevent the damage of heater.

Two copper-constantan thermocouples (Type-J) were imbedded in the copper cylinder to measure the surface temperature of the heater. They were positioned at the (0.15) m and (0.25) m from the bottom of the heater respectively. A (0.005) m long Teflon cone was attached to the bottom of the heater. Its purpose was to promote a fully developed thermal boundary layer at the heater surface and to prevent eddies.

Thermocouples were connected to an interface system. The local bed temperature (Bulk temperature) was taken by averaging five measurements continuously for each run. These temperature measurements were recorded after ensuring that steady-state was reached (i.e. monitoring the variation of the temperatures with time).

Results and Discussions

The model of series thermal resistances is used to characterize the resistance in the fluidized bed. The overall heat transfer coefficient in the bed depends on the effective radial thermal conductivity (k_{er}) and the apparent surface heat transfer coefficient (h_s). In the present liquid-liquid-solid fluidized beds, the existence of radial temperature profile in the region adjacent to the heater surface and that in the bed interior indicates that two resistances connected in series can be represented by a series thermal resistance model.

Heat Transfer Coefficient

The heat transfer coefficient (h) between the immersed heater and the bed can be influenced by the resultant flow behavior of dispersed droplet, fluidized particles and the continuous medium. Thus, the effect of individual flow behavior on the heat transfer coefficient has been determined. The overall heat transfer coefficients (h) calculated from experimental measurements of temperature differences are plotted versus the velocity of dispersed liquid for various values of continuous liquid velocities.

Figures (4-7) show these plots for different values of heat flux from the heater. It is shown clearly that the heat transfer coefficient generally increases with both u_c and u_d . The corresponding values of h at the same values of u_c and u_d show an increasing trend with the increase of heat flux from the heater. This increase in h values can be attributed to the effect of heating level on the physical properties of both dispersed and continuous liquids in the bed.

Figures (8-11) present the experimental values of overall heat transfer coefficients versus continuous liquid velocity for various dispersed liquid velocities for different heat fluxes from the heater. These plots show the existence of a maximum in heat transfer coefficient at certain values of u_c and u_d . As can be seen, h exhibits its maximum value with a variation of u_c . In the relatively lower range of u_c , turbulence intensity in the bed increases with increasing u_c ; however turbulence intensity decreases with a further increase in u_c due to the reduction of solids holdup in the bed.

Since the bed porosity is a proportional function of u_c , the variation of h with u_c is very similar to that with bed porosity, as can be seen in Fig.(12). The maximum value of heat transfer coefficient with respect to bed porosity can be attributed to the variation of effective turbulence related to solid phase holdup in the beds. The turbulence intensity attains its optimum value for heat transfer at the intermediate bed porosity and the

corresponding continuous liquid-phase velocity conditions.

Figure (12) shows a comparison between the results of the present study with the previous studies. Baker et al. (1978) used high density particles (2450 kg/m^3) as fluidized beds in gas-liquid-solid system in a (0.24) m diameter column, and Kim et al. (1999) studied the effect of bed porosity on heat transfer coefficient in liquid-liquid-solid fluidized bed system using particles of density (2500 kg/m^3) and (0.102) m column diameter. The deviation in the result is normal since the experimental conditions are different for each work regarding the particle sizes, particle densities and column diameters.

Correlation of Experimental Results

The heat transfer in the three-phase fluidized beds is mainly affected by the heat transfer coefficient near the heater surface region which is controlled by conduction through the liquid boundary layer covering the heater surface. In the liquid-liquid-solid fluidized beds the heat transfer coefficient is considerably affected by the liquid velocity. The dispersed phase velocity has additional effect on the heat transfer coefficient. Good representation of the experimental results in the present study can be attained by the following equation:

$$Nu = 0.164 (Re_l Pr)^{1.56} (Re_d)^{4.05} (1-e)^{6.96}$$

The correlation coefficient is (0.93), and standard deviation is (33.0).

Conclusions

1. The heat transfer coefficient (h) between the immersed heater and the bed is strongly influenced by the resultant flow behavior of dispersed phase, fluidized particles and the continuous medium.
2. The heat transfer coefficient generally increases with both u_c and u_d . The corresponding values of the coefficient at the same values of u_c and u_d show an increasing trend with the increase of heat flux from the heater.
3. The heat transfer coefficient in liquid-liquid-solid fluidized beds can be correlated in terms of the following dimensionless groups.

$$Nu = 0.164 (Re_l Pr)^{1.56} (Re_d)^{4.05} (1-e)^{6.96}$$

References

- [1]. Abdul – Wahab M .I. , “ Hydrodynamics and Temperature Distribution in Low Density Particles Fluidized Beds Using the Finite Element Technique ”, Ph.D. Thesis, University of Baghdad, 1997.
- [2]. Baker, C.G.J., Armstrong, E.R., and Bergougnon, M. A., “Heat Transfer in Three - Phase Fluidized Beds”, Powder Technology, 21, 195-204, 1978.
- [3]. Dakshinamurty, P . , Subrahmanyam, V., Prasada Rao Rv, and Vijayasradhi, P., , “ Liquid-Liquid-Solid Mass Transfer in 3-Phase Fluidized Beds. 3. Measurement of Individual Fluid – Phase Resistances ”, Ind. Eng. Chem. Proc. Des. Dev. , 23, 132-137, 1984.
- [4]. Dakshinamurty, P. , Veerabhadrarao, K. , and Venkatarao, A.B., “ Bed Porosities in Three Phase (Liquid-Liquid) Fluidized Beds ”, Ind. Eng. Chem. Pro. Des. Dev., 18 , 638-640, 1979.
- [5]. Kim, S.D., Kim, D.Y. and Han, J.H., “ Dispersed Phase Characteristics in Three Phase (Liquid – Liquid – Solid) Fluidization Beds ”, Can. J. Chem. Eng., 72, 222-228, 1994.
- [6]. Kim, S. D., Lee, M.J., and Han, J. H. “ Axial Dispersion Characteristics of Three (Liquid – Liquid – Solid) Phase Fluidized Beds ”, Can. J. Chem. Eng., 67,276-282, 1989.
- [7]. Kim S. D., Yu. Y.H. and Hahn, P.W., “ Phase Holdups and Liquid-Liquid extraction in Three - Phase Fluidized Beds ”, Chem. Eng. Comm., 68, 57- 68, 1988.
- [8]. Kim, S.D., Kim, J.S., Nam., C.H., Kim., S.H. and Kang, Y. “ Immersed Heater – to – Bed Heat Transfer in Liquid – Liquid – Solid Fluidized Beds ”, Chem. Eng. Sci., 54, 5173-5179, 1999.
- [9]. Tang, W.T. and Fan, L.S. “ Axial Liquid Mixing in Liquid – Solid and Gas – Liquid – Solid Fluidized Beds Containing Low Density Particles. Chem. Eng. Sci., 45, 543-548, 1990.
- [10]. Van Zeen “ Hydrodynamics of a Liquid – Liquid – Solid Fluidized Bed Bioreactor ”, Ph.D. Thesis Wageningen University, the Netherlands, 2003.

Table (1) Physical Properties of the Continuous and Dispersed Phases

Liquid Phase	Density, (kg/m ³)	Viscosity, (m Pa. s)	Thermal Conductivity, (W/m K)	Heat Capacity [C _p ×10 ⁻³], (J/kg K)
Water	1000	1.0	0.60	4.18
Kerosene	780	2.5	0.15	2.10

**Figure (1) General Arrangement of the Experimental Setup**

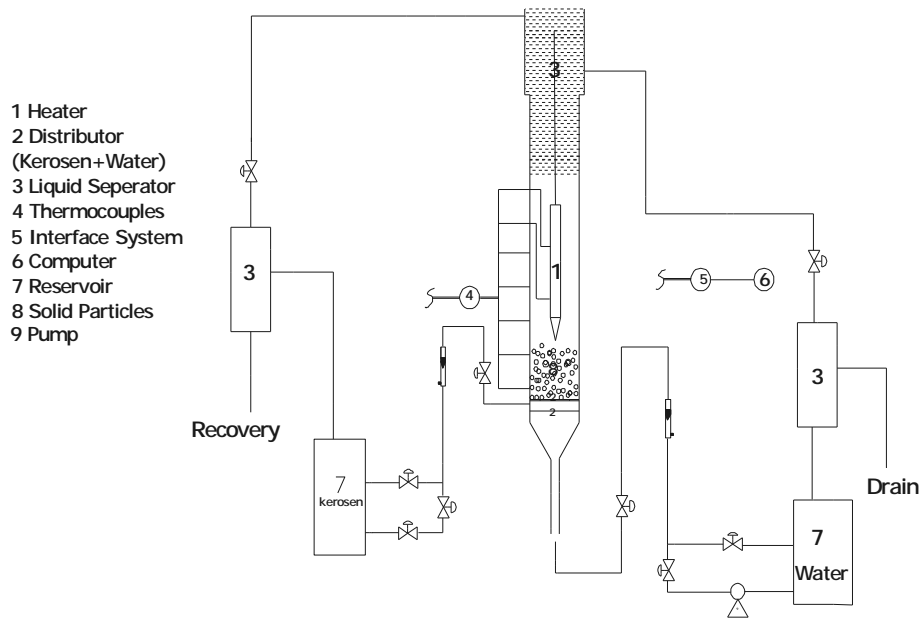


Figure (2) Schematic Diagram of the Experimental Setup

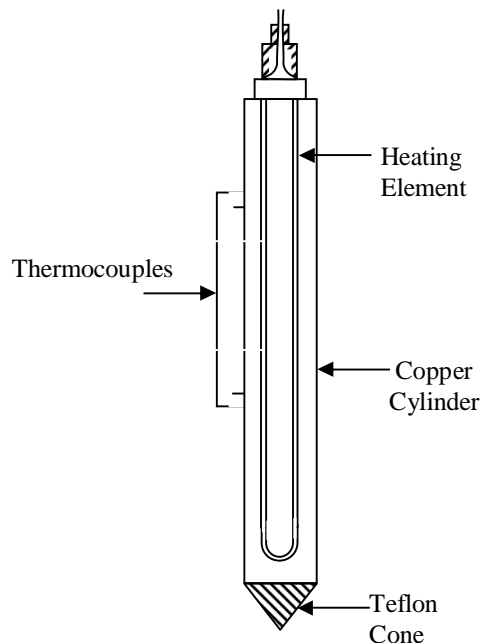


Figure (3) The Heater Assembly

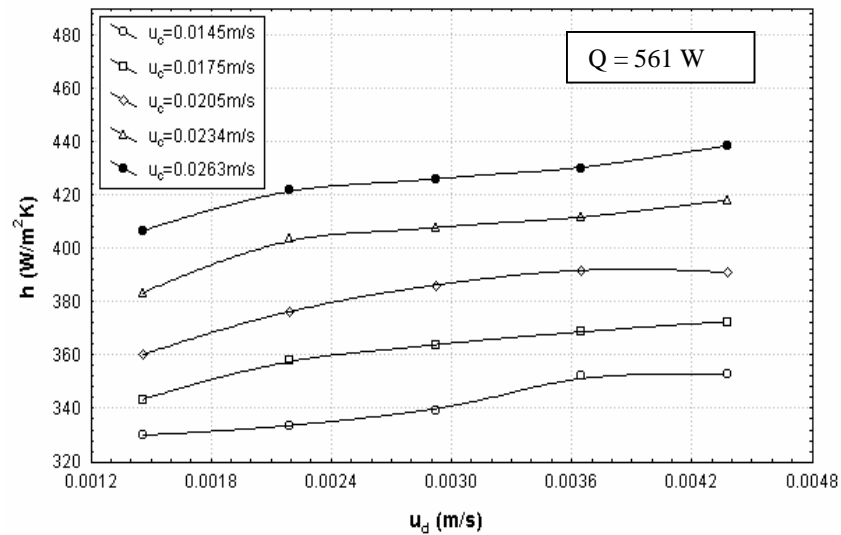


Figure (4) Variation of Overall Heat Transfer Coefficient with u_c and u_d

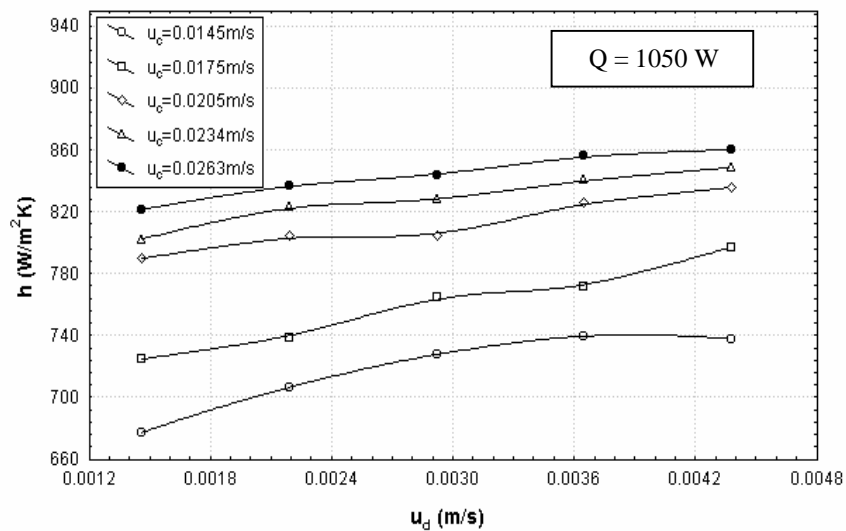


Figure (5) Variation of Overall Heat Transfer Coefficient with u_c and u_d

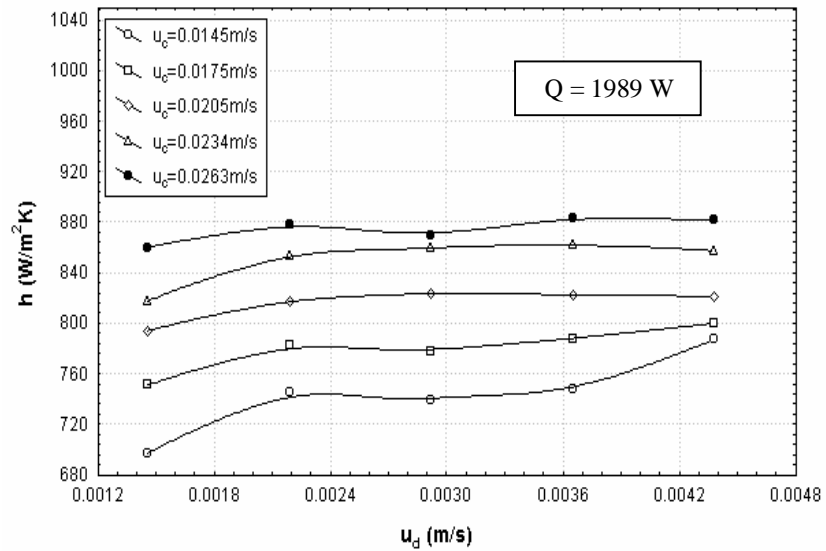


Figure (6) Variation of Overall Heat Transfer Coefficient with u_c and u_d

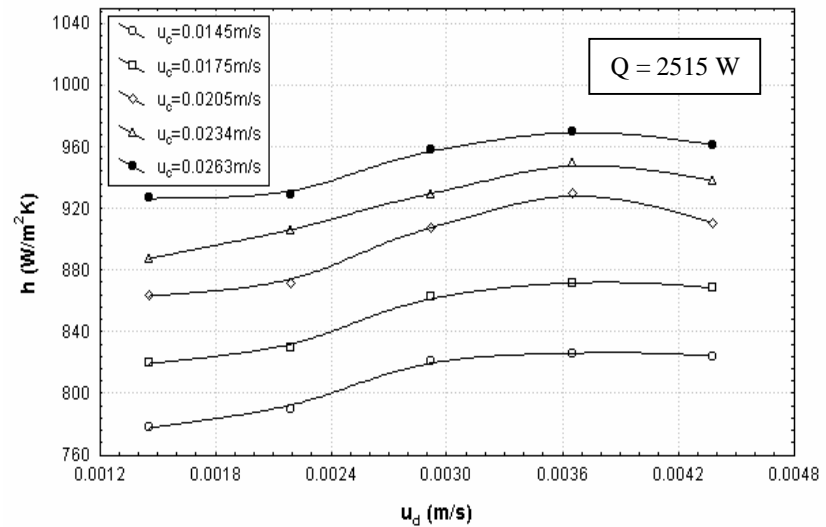


Figure (7) Variation of Overall Heat Transfer Coefficient with u_c and u_d

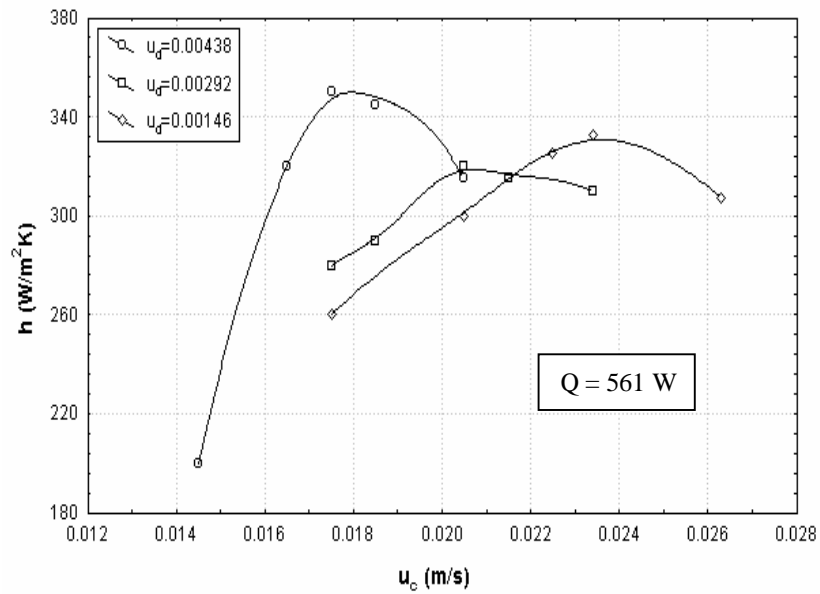


Figure (8) Heat Transfer Coefficient vs. Continuous Phase Velocity for Different Values of u_d

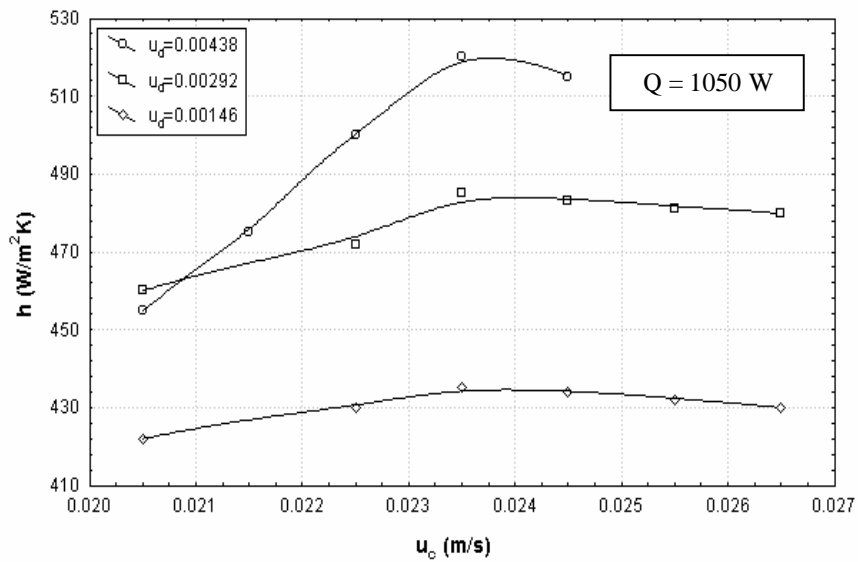


Figure (9) Heat Transfer Coefficient vs. Continuous Phase Velocity for Different values of u_d

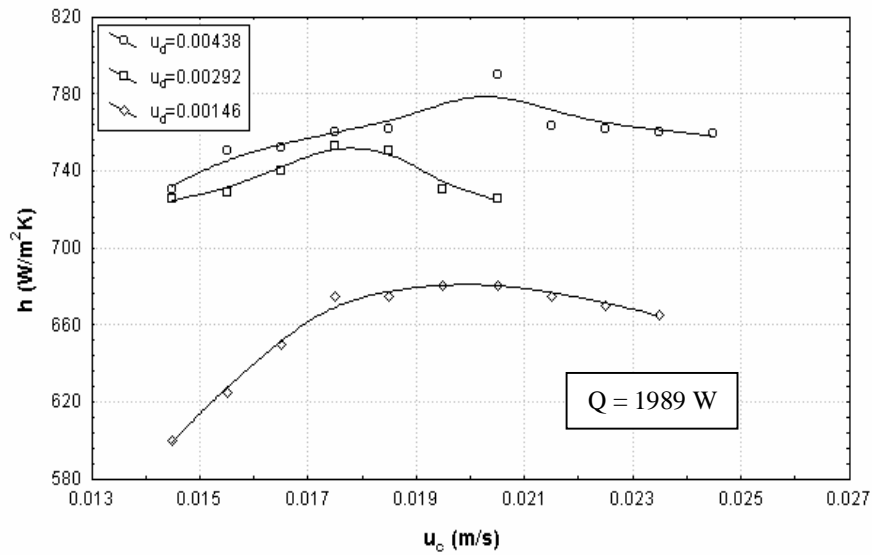


Figure (10) Heat Transfer Coefficient vs. Continuous Phase Velocity for Different values of u_d

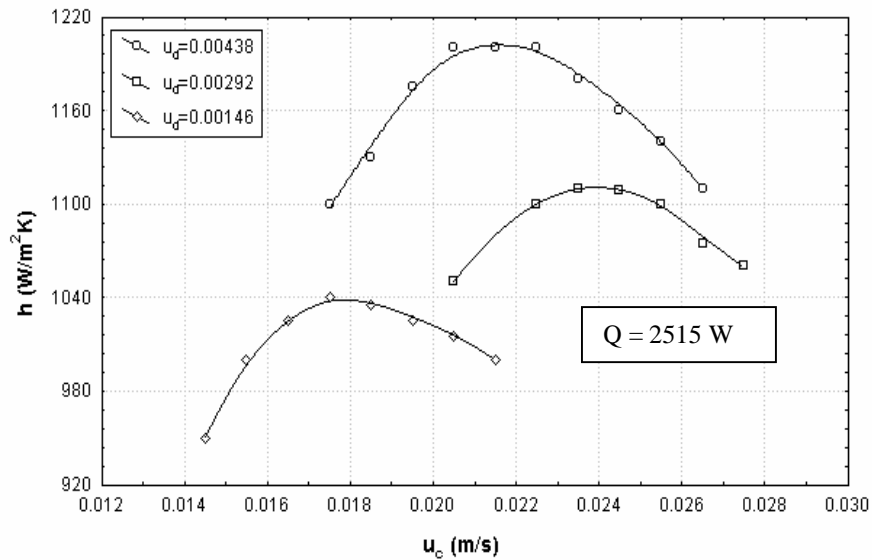


Figure (11) Heat Transfer Coefficient vs. Continuous Phase Velocity for Different values of u_d

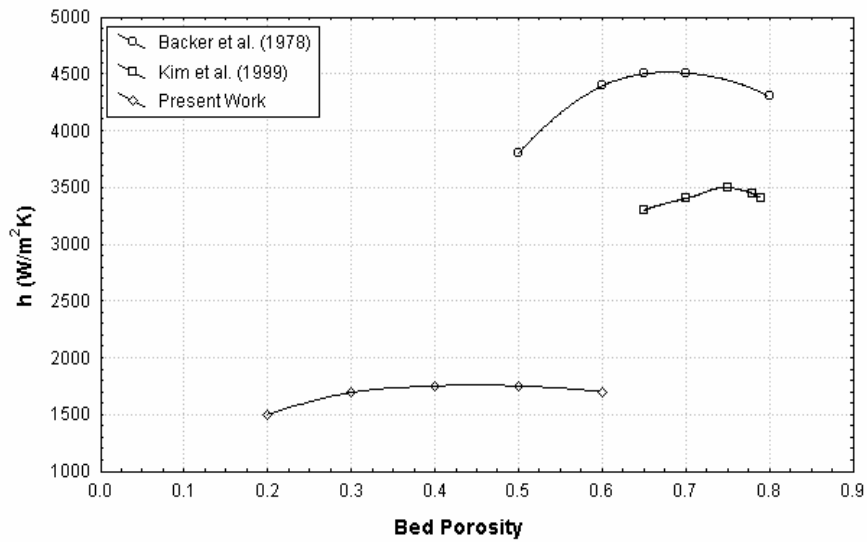


Figure (12) Overall Heat Transfer Coefficient vs. Bed Porosity Compared with Previous Studies